ISSN 0030-400X, Optics and Spectroscopy, 2016, Vol. 121, No. 1, pp. 25–31. © Pleiades Publishing, Ltd., 2016.
Original Russian Text ©A.A. Sobol, V.E. Shukshin, A.I. Zaitsev, 2016, published in Optika i Spektroskopiya, 2016, Vol. 121, No. 1, pp. 28–35.

CONDENSED-MATTER SPECTROSCOPY

Raman Spectroscopy of SrB_4O_7 Single Crystals in the Temperature Range 300–1273 K

A. A. Sobol[a], **V. E. Shukshin**[a], **and A. I. Zaitsev**[b]

[a] *Prokhorov General Physics Institute, Russian Academy of Sciences, Moscow, 119991 Russia*
[b] *Kirenskii Institute of Physics, Siberian Branch, Russian Academy of Sciences, Krasnoyarsk, 660036 Russia*
e-mail: sobol@lst.gpi.ru, shukshinve@lst.gpi.ru

Received January 22, 2016

Abstract—The polarized Raman spectra of SrB_4O_7 (SBO) single crystals are studied in detail in the temperature range of 300–1273 K. The *TO*, *LO*, and *IO* phonon lines of A_1, A_2, B_1, and B_2 symmetries of rhombic SBO at 300 K are identified. The behavior of the Raman spectra of SBO crystals is studied upon heating up to their melting. The relation of Raman spectra with the structure of boron–oxygen fragments, as well as the transformation of spectra in the process of melting of SBO crystals, is discussed.

DOI: 10.1134/S0030400X16070201

INTRODUCTION

Crystals with the structure of the stable modification of strontium diborate SrB_4O_7 (SBO) have been known for a long time [1, 2]. The structure of these crystals belongs to the rhombic syngony with the $Pnm2_1$ space group and has some specific features. This structure is based on a three-dimensional lattice formed only from boron–oxygen tetrahedra, some of the structural positions of which contain oxygen linked to three borons [3].

SBO single crystals attract an attention due to a combination of unique properties, namely, the fundamental absorption edge at a record-short wavelength (~130 nm) among oxide materials and high nonlinear optical coefficients [2, 4, 5]. Recently [6], continuously tunable lasing in these crystals was obtained at wavelengths up to 121 nm [6].

The authors of [7] analyzed the possibility of the occurrence of a paraelectric form of SrB_4O_7 at high temperatures, which could be caused by a second-order phase transition. This phase transition is undetectable by differential thermal analysis, while the paraelectric phase cannot be retained at 300 K even by fast quenching to study it by X-ray diffraction. Therefore, to detect this phase transition, it is necessary to perform experiments directly at high temperatures. Raman spectroscopy has previously been successfully used to detect phase transformations and identify paraelectric phases in such oxide crystals as $LiNbO_3$, $KTiOPO_4$, and $LaNbO_4$ [8–10]. It is this method that is used in the present work to study a possible temperature phase transition in SrB_4O_7 single crystals.

The polarized Raman spectra and the identification of the symmetry of vibrational modes in the SrB_4O_7 single crystal at 300 K were previously disclosed in [7]. However, this work contained some inaccuracies related to the absence of complete experimental information on the Raman spectrum of this material. In particular, the Raman spectra of SrB_4O_7 were recorded only in the 90° geometry, which restricted the analysis of vibrational modes. In addition, the Raman spectra of SrB_4O_7 in work [7] were studied in the frequency range below 1000 cm^{-1}, while these spectra in borate crystals are known to extend to at least 1300 cm^{-1}. In this connection, in the present work we studied in detail the Raman spectra of SrB_4O_7 single crystals at 300 K and identified the symmetry of almost all the transverse and longitudinal vibrational modes, which was not done in previous studies.

OBJECTS AND METHODS OF INVESTIGATION

The SrB_4O_7 crystal was grown by the Czochralski method from a stoichiometric melt. The synthesis conditions and details are presented in [11]. The sample for investigation of the Raman spectra was prepared in the form of a parallelepiped with planes oriented according to the *a*, *b*, and *c* axes by the X-ray diffraction method. Strontium diborate has the rhombic structure $Pnm2_1$ (C_{2v}^7) [7] with two formula units in the unit cell. This symmetry implies the presence of 72 vibrations corresponding to the wave vector with $k = 0$, namely, $19A_1 + 17A_2 + 17B_1 + 19B_2$, including acoustic vibrations $A_1 + B_1 + B_2$. The vibrations of the

Table 1. Scattering geometries used for identification of phonon in the rhombic SrB_4O_7 structure at 300 K. The *X*, *Y*, and *Z* directions correspond to the [100], [010], and [001] crystallographic axes of the crystal

Scattering geometry	Vibration symmetry	Observed scattering tensor component
$X(ZZ)\bar{X}$	$A_1(TO)$	α_{zz}
$X(ZZ)Y$	$A_1(TO)$	α_{zz}
$Y(XX)\bar{Y}$	$A_1(TO)$	α_{xx}
$X(YY)\bar{X}$	$A_1(TO)$	α_{yy}
$Z(XX)\bar{Z}$	$A_1(LO)$	α_{xx}
$Z(YY)\bar{Z}$	$A_1(LO)$	α_{yy}
$Z(XY)\bar{Z}$	A_2	α_{xy}
$Y(XY)Z$	A_2	α_{xy}
$Z(XZ)Y$	$B_1(TO)$	α_{xz}
$X(ZX)Y$	$B_1(TO)$	α_{zx}
$Z(YZ)X$	$B_2(TO)$	α_{yz}
$Y(ZY)X$	$B_2(TO)$	α_{zy}

A_1, B_1, and B_2 symmetries are active in both Raman and IR spectra, while the vibration of the A_2 symmetry is active only in the Raman spectra. In this connection, in addition to 69 transverse *TO* vibrations $18A_1 + 17A_2 + 16B_1 + 18B_2$, the Raman spectra may also exhibit longitudinal *LO* vibrations of the A_1, B_1, and B_2 symmetries, when propagation vector **k** of scattered phonons coincides with the corresponding *a*, *b*, and *c* axes of the crystal. Along with pure *TO* and *LO* phonon lines, the Raman spectra should contain the lines of intermediate *IO* phonons when vector **k** is directed at an angle to the crystallographic axes. This phenomenon is typical for the use of so-called "normal scattering geometries," in which the directions of the incident and scattered beams are perpendicular to each other. Raman spectra at 300 K were recorded on a Spex-Ramalog 1403 monochromator with a spectral slit width of 1 cm^{-1}. The Raman spectra were excited by a cw argon laser with wavelengths of 488.0 and 514.5 nm and an average power of 0.6 W. The Raman spectra excited at different laser wavelengths showed no luminescence of foreign impurities in the samples in the spectral range studied.

Raman spectra at temperatures up to 1300 K were measured using a specially designed setup [12]. As an excitation source, we used a copper vapor laser with a wavelength of 578.2 nm operating in a repetitively pulsed regime with a repetition rate of 15 kHz and an average power of 5 W. The Raman spectra upon heating and melting of samples were studied in air in platinum crucibles in a vertical tube resistance furnace made of Pt-30%Rh wire. The temperature was mea-

Table 2. Frequencies (cm^{-1}) of vibrations corresponding to *TO*, *LO*, and *IO* phonons in the Raman spectrum of the SrB_4O_7 crystal at 300 K

A_1					A_2	B_1		B_2	
α_{xx}		α_{yy}		α_{zz}	α_{xy}/α_{yx}	α_{xz}/α_{zx}		α_{yz}/α_{zy}	
TO	*LO*	*TO*	*LO*	*TO*	*TO*	*TO*	*IO*	*TO*	*IO*
–	–	104	105	104	109	–	148	117	117
151	183	151	183	153	156	160	193	142	150
282	282	282	282	282	237	231	233	301	303
294	294	294	294	294	263	282	282	408	417
362	364	362	365	362	324	444	444	449	449
431	431	431	431	431	416	513	514	517	517
491	491	491	491	491	500	557	557	555	558
580	580	580	580	580	518	609	609	634	635
634	634	634	634	634	535	650	650	726	730
641	652	–	652	–	557	781	783	814	814
705	708	705	708	705	616	890	890	893	914
741	809	741	799	741	720	930	930	938	954
807	843	807	842		753	969	978	962	961
885	–	885	902	885	799	1012	1042	1055	1056
989	1091	989	1091	989	926	1068	1144	1093	1151
1042	1043	–	–	–	997	1138	1307	1169	1301
1148	1234	–	1234	–	1167				

α_{ij} denote scattering tensor components determining the intensity of Raman lines for the studied scattering geometries from Table 1.

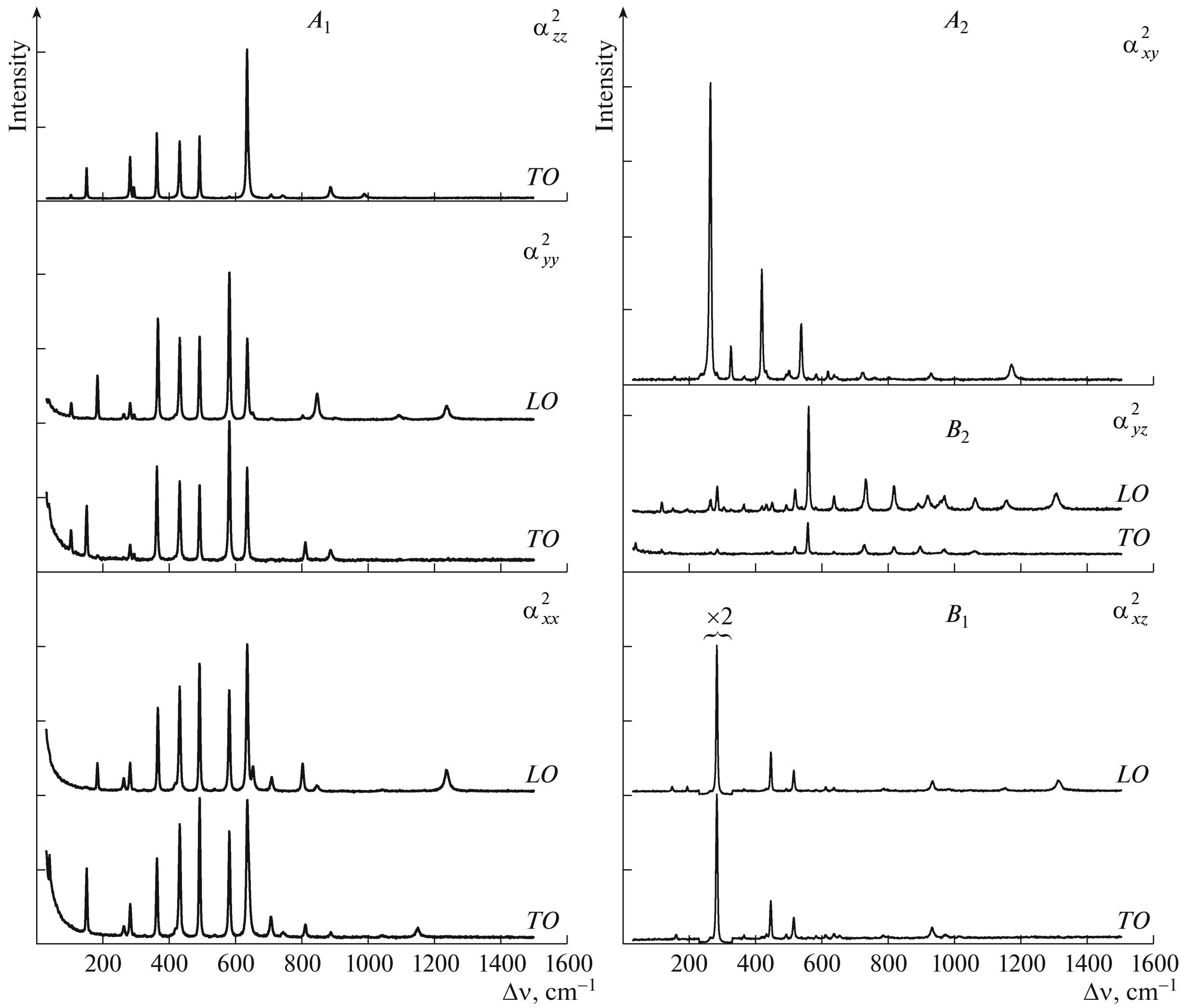

Fig. 1. Polarized Raman spectra of SrB_4O_7 single crystal at 300 K in the scattering geometries corresponding to the *TO*, *LO*, and *IO* modes of A_1, A_2, B_1, and B_2 symmetries (α^2_{ij} correspond to the scattering tensor components from Table 1).

sured with an accuracy of 1 K by a Pt-6%Rh–Pt-30%Rh thermocouple contacting the crucible. To study the melt, the Raman spectra were recorded and excited through its top surface. The Raman spectra at high temperatures were recorded with a resolution of 3–4 cm^{-1}.

EXPERIMENTAL RESULTS AND DISCUSSION

For polarization investigations, we used 12 (both 90° and 180°) scattering geometries, which are presented in Table 1. This allowed us to reliably identify *TO* vibrations, as well as *LO* and *IO* vibrations of the A_1, B_1, and B_2 symmetries, which was not done in [7]. The Raman spectra of the SrB_4O_7 crystal at 300 K, which illustrate the vibrational spectra of *TO*, *LO*, and *IO* phonons with the A_1, B_1, B_2, and A_2 symmetries at 300 K, are shown in Fig. 1. The Raman spectra recorded at 300 K in the high-frequency range of 800–1400 cm^{-1} are shown in more detail in Fig. 2. Table 2 lists the frequencies of these phonons. We identified $17A_1 + 17A_2 + 15B_1 + 16B_2$ *TO* vibrations. The vibrations in Table 2 were identified without taking into account the frequencies of weak lines that were observed in the spectra of some geometries but were traces of intense lines from the spectra of another scattering geometry. This eliminated an erroneous assignment of one frequency simultaneously to Raman lines of different symmetries. In our investigations, the positions of strong *TO* lines were observed to coincide only once, in the case of the 282-cm^{-1} line in the A_1 and B_1 symmetries. This case will be considered below in studying the temperature behavior of Raman spectra.

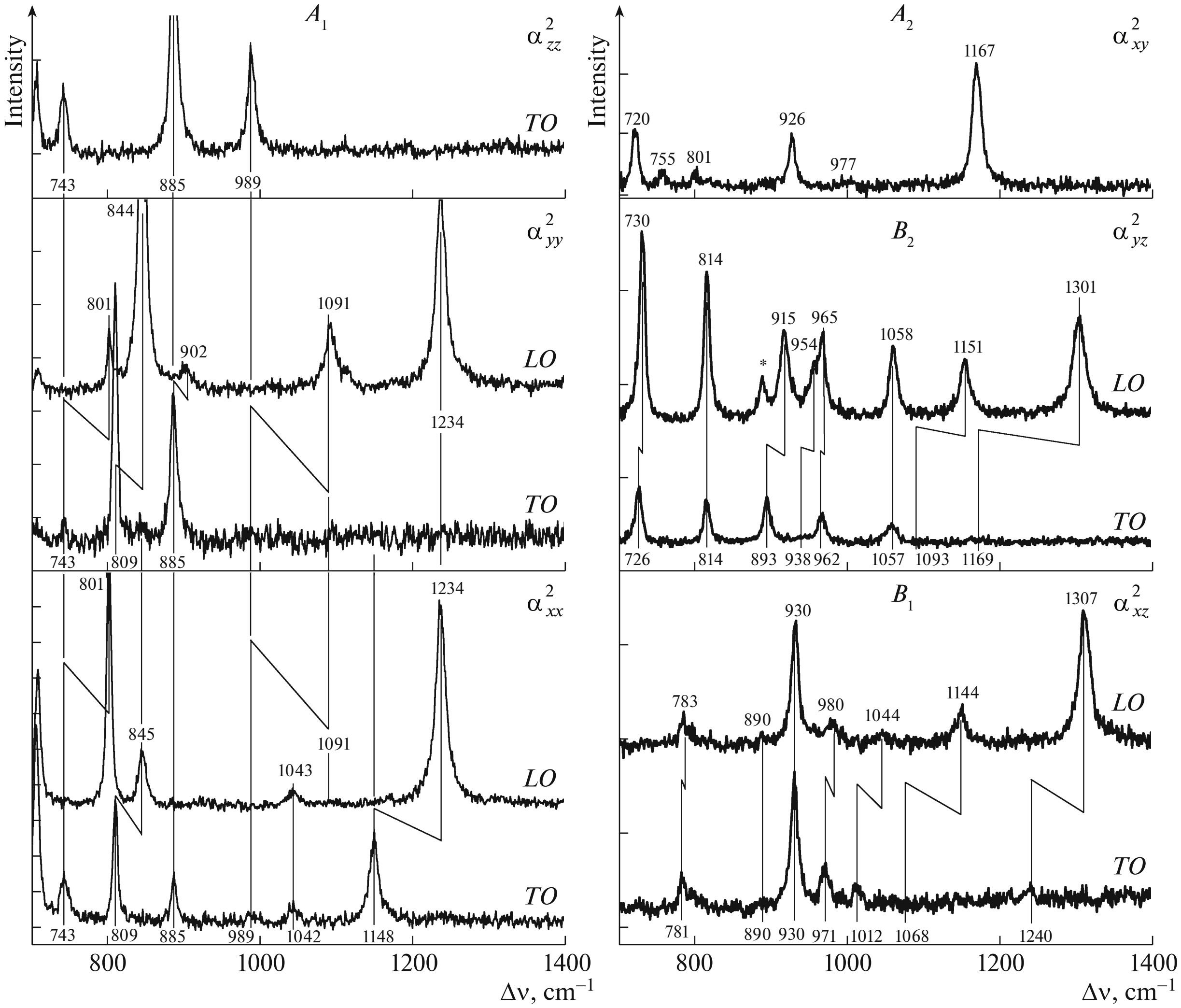

Fig. 2. High-frequency (700–1400 cm^{-1}) region of polarized Raman spectra of SrB_4O_7 single crystal at 300 K. *Denotes lines forbidden in the given scattering geometry.

Analysis of the spectra of *LO* and *IO* vibrations revealed some interesting effects. The frequency shift of these vibrations with respect to the corresponding *TO* vibrations in the region of low and medium frequencies was either absent or did not exceed 10 cm^{-1}, while this shift in the high-frequency spectral range reached 160 cm^{-1} (Figs. 1, 2).

In the Raman spectra corresponding to the *LO* and *IO* vibrations of the SrB_4O_7 crystal, we observed the influence of the electrooptic effect on the intensities of lines compared to their intensities in the scattering geometries for *TO* phonons. Previously, this phenomenon has been observed in α-quartz [13], lithium niobate [14], and LiB_3O_5 [15] crystals, and we illustrate this effect in SrB_4O_7 crystals by the Raman spectra in the region of low-frequency shifts (Fig. 3).

The frequency shifts and the changes in the intensity of Raman lines for A_1 vibrations in the scattering geometries for *TO* and *LO* phonons allowed us to identify A_1 vibrations in the frequency shift range of 620–660 cm^{-1} (Fig. 3). The Raman spectrum in the scattering geometries corresponding to tensor components α_{zz} and α_{yy} for $A_1(TO)$ vibrations exhibited only one line with a frequency of 634 cm^{-1}. In scattering geometry α_{xx}, we recorded a high-frequency wing of this line, which implies the existence of two $A_1(TO)$ lines in this spectral range. The Raman spectra recorded in geometries for $A_1(LO)$ phonons clearly demonstrate the presence of just two well-resolved lines of A_1 vibrations in the frequency shift range of 630–650 cm^{-1}. The increase in the intensities of vibrational lines of particular symmetries when passing from *TO* phonons to *LO* or *IO* phonons allowed us to

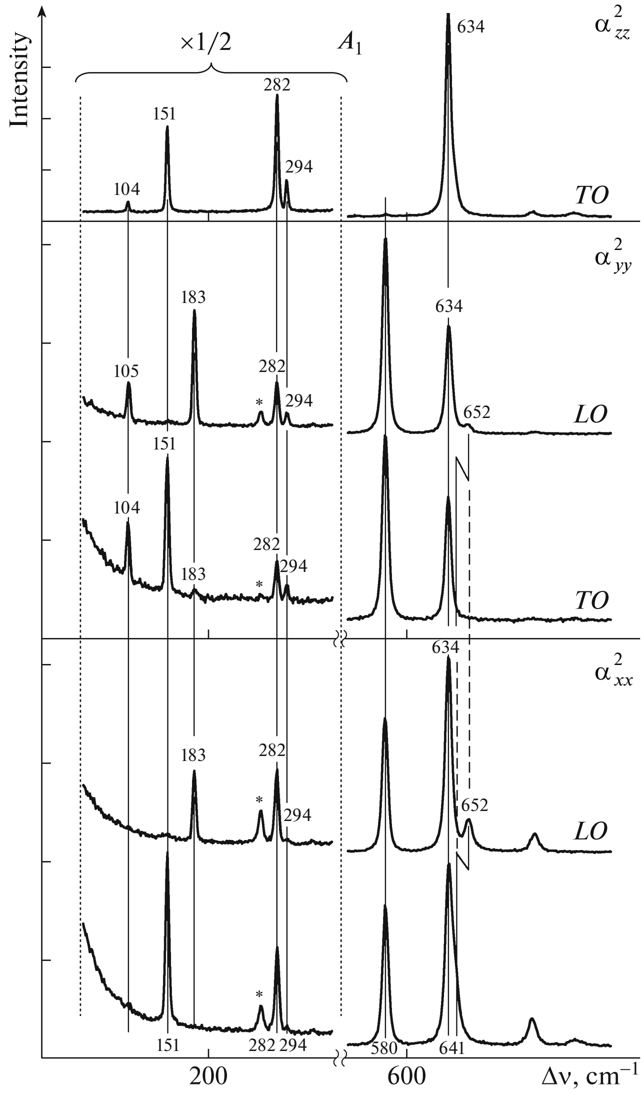

Fig. 3. Low-frequency (50–700 cm^{-1}) region of polarized Raman spectra of SrB_4O_7 single crystal at 300 K. * denotes lines forbidden in the given scattering geometry.

note the existence of extremely weak lines of *TO* vibrations of the B_1 and B_2 symmetries in the high-frequency region (Fig. 2).

The authors of [7] calculated a model of a high-temperature paraelectric phase for SrB_4O_7, which was supposed to have the structure *Pnmm* (D^1_{2h}). In this case, the phase transition temperature had to exceed the melting temperature of strontium diborate.

To check the possibility of this transition, we studied the Raman spectra in the processes of heating of the stable form of SrB_4O_7 single crystal up to its melting temperature. These Raman spectra are shown in Fig. 4. In the experiment, it was possible to record the lines of the $A_1(TO) + B_1(TO)$ vibrations due to the use of the scattering geometry $\{Y(ZZ)\overline{Y} + Y(ZX)\overline{Y}\}$ (without an analyzer). From Fig. 4, it is seen that the Raman spectrum noticeably changes only at a temperature of 1273 K (curve *6*). It was visually observed that the crystal melts at this temperature. At the same time, the Raman spectra in the temperature range of 300–1268 K testify to the absence of phase transformations in the studied SrB_4O_7 crystal, at least to a temperature of 5 degrees below the melting point. The phase transition $Pnm2_1$ (C^7_{2v}) → *Pnmm* (D^1_{2h}) suggested in [7], at which the number of formula units does not change, should be accompanied by at least twofold decrease in the number of lines in the Raman spectra of the suspected paraelectric phase due to the existence of an inversion center in its unit cell (alternative prohibition rule). However, spectra *1–5* in Fig. 4 demonstrate only a broadening and a red shift with increasing temperature, which is a common consequence of anharmonicity effects. The Raman spectrum of the molten crystal at 1273 K (curve *6* in Fig. 4) consists of broad bands, which, according to the results of previous experiments on the Raman spectra of borate melts [16–18], can be assigned to internal vibrations of boron–oxygen complexes in the molten state. A spectrum of these internal vibrations can also be separated in crystalline SrB_4O_7, but, taking into account the complex structure of SrB_4O_7, this is rather difficult to do at present. The Raman spectrum of the melt slowly cooled to 300 K contained only the lines of the initial SrB_4O_7 single crystal (curve *7* in Fig. 4), which testified to the absence of phase transformations during cooling as well. Since this cooling led to the formation of a polycrystalline sample, its Raman spectrum at 300 K contained the lines of both *TO* and *LO* vibrations of all the four phonon symmetries.

The study of temperature-induced changes in the Raman spectra of the SrB_4O_7 single crystal allowed us to clarify the nature of the 282-nm band at 300 K. According to the polarization investigations at 300 K, this frequency should belong to two intense vibrational lines with the symmetries $A_1(TO)$ and $B_1(TO)$ (Table 2). As is seen from Fig. 4 (curves *1–5*), due to different temperature dependences of the frequencies of these vibrations, they become well resolved in the Raman spectra at a high temperature. This effect was previously observed in the Raman spectra of $CaWO_4$ [19] and monoclinic HfO_2 [20].

CONCLUSIONS

On the basis of detailed studies of polarized Raman spectra in different scattering geometries, we identified $17A_1 + 17A_2$ *TO* vibrations predicted by group-theoretical analysis. From $16B_1 + 18B_2$ *TO* vibrations, which should be observed in the Raman spectra of SrB_4O_7, we observed $15B_1 + 16B_2$ vibrations. We can suggest the presence of the sixteenth *TO* vibration of

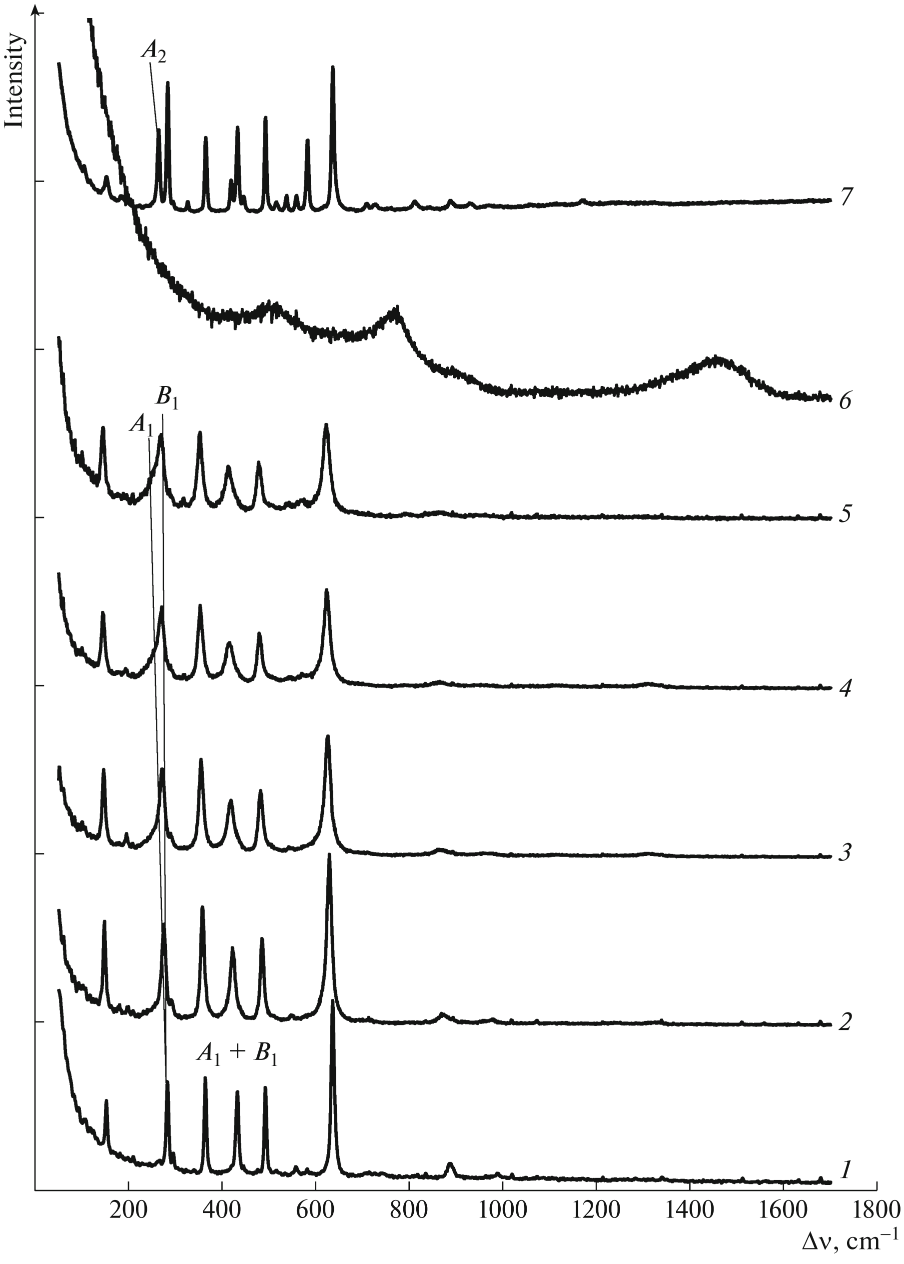

Fig. 4. Evolution of Raman spectra upon heating an oriented SrB_4O_7 single crystal from 300 K to the melting temperature (scattering geometry $Y(ZZ)\overline{Y} + Y(ZX)\overline{Y}$). The spectra are measured at temperatures of (*1*) 300, (*2*) 873, (*3*) 1073, (*4*) 1173, (*5*) 1268, (*6*) 1273 (melt), and (*7*) 300 K (cooled melt).

the B_1 symmetry in the region below 150 cm^{-1}, because just 16 lines were observed for *IO* phonons of this symmetry (Table 2). Therefore, these data confirm the conclusion of X-ray diffraction analysis about the rhombic lattice symmetry *Pnm*2$_1$ (C_{2v}^7) of the SrB_4O_7 crystal.

The frequency shift of *LO* vibrations with respect to corresponding *TO* vibrations is most pronounced in the high-frequency region and can reach 160 cm^{-1}.

It is found that the electrooptic effect causes a change in the intensities of the Raman lines of *LO* vibrations in comparison with the corresponding *TO* vibrations.

The high-temperature investigations of Raman spectra did not confirm the existence of a ferro-paraelectric phase transition in the SrB_4O_7 crystal structure.

Comparing the Raman spectra of the SrB_4O_7 crystal before melting with the spectrum of its melt, we can conclude that, although boron–oxygen complexes exist in molten strontium diborate, their structure has nothing in common with the structure of boron–oxygen fragments in the specific crystal lattice of SrB_4O_7.

ACKNOWLEDGMENTS

This work was supported by the Russian Foundation for Basic Research, project no. 13-02-00707a.

REFERENCES

1. J. Krogh-Moe, Acta Chem. Scand. **18**, 2055 (1964).
2. S. Block, A. Perloff, and C. E. Weir, Acta Crystallogr. **17**, 314 (1964).
3. F. Pan, G. Shen, R. Wang, X. Wang, and D. Shen, J. Cryst. Growth **241**, 108 (2002).
4. K. Machida, H. Hata, K. Okuno, G. Adachi, and J. Shiokawa, J. Inorg. Nucl. Chem. **41**, 1425 (1979).
5. H. Huppertz, Z. Naturforsch. B **58**, 257 (2003).
6. P. Trabs, F. Noack, A. S. Aleksandrovsky, A. I. Zaitsev, and V. Petrov, Opt. Lett. **41**, 618 (2016).
7. V. I. Zinenko, M. S. Pavlovskii, A. I. Zaitsev, A. S. Krylov, and A. S. Shinkarenko, J. Exp. Theor. Phys. **115**, 455 (2012).
8. Yu. K. Voron'ko, A. B. Kudryavtsev, V. V. Osiko, and A. A. Sobol', Fizika Tverdogo Tela **29**, 1348 (1987).
9. Yu. K. Voron'ko, V. A. D'yakov, A. B. Kudryavtsev, V. V. Osiko, A. A. Sobol', and E. V. Sorokin, Fizika Tverdogo Tela **31**, 150 (1989).
10. G. V. Anan'eva, A. M. Korovkin, A. B. Kudryavtsev, A. K. Kupchikov, A. I. Ryskin, and A. A. Sobol', Fizika Tverdogo Tela **23**, 1079 (1981).
11. A. I. Zaitsev, A. S. Aleksandrovsky, A. D. Vasiliev, and A. V. Zamkov, J. Cryst. Growth **310**, 1 (2008).
12. Yu. K. Voron'ko, A. B. Kudryavtsev, V. V. Osiko, and A. A. Sobol', in *Growth of Crystals,* Ed. by Kh. S. Bagdasarov and E. L. Lube (Consultant Bureau, New York, 1991), Vol. 16, p. 199.
13. J. D. Masso, C. A. She, and D. F. Edwards, Phys. Rev. B **1**, 4179 (1970).
14. A. S. Barker, Jr. and R. Loudon, Phys. Rev. **158**, 433 (1967).
15. Yu. K. Voron'ko, A. A. Sobol', and V. E. Shukshin, Opt. Spectrosc. **115**, 863 (2013).
16. Yu. K. Voron'ko, A. V. Gorbachev, A. B. Kudryavtsev, and A. A. Sobol', Neorg. Mater. **28**, 1361 (1992).
17. Yu. K. Voron'ko, A. V. Gorbachev, A. B. Kudryavtsev, and A. A. Sobol', Neorg. Mater. **28**, 1368 (1992).
18. Yu. K. Voronko, A. V. Gorbachov, V. V. Osiko, A. A. Sobol, R. S. Feigelson, and R. K. Route, J. Phys. Chem. Solids **54**, 1579 (1993).
19. A. F. Banishev, Yu. K. Voron'ko, A. B. Kudryavtsev, V. V. Osiko, and A. A. Sobol', Kristallografiya **27**, 618 (1982).
20. Yu. K. Voron'ko, A. A. Sobol', and V. E. Shukshin, Phys. Solid State **49**, 1963 (2007).

Translated by M. Basieva